

1 ***Plasmodium falciparum* growth is regulated by Sphingosine 1 phosphate**
2 **produced by Host Erythrocyte Membrane Sphingosine kinase 1**

3

4

5 **Raj Kumar Sah¹, Monika Saini¹⁻², Soumya Pati² and Shailja, Singh^{1*}**

6

7 ¹Special Centre for Molecular Medicine, Jawaharlal Nehru University, New
8 Delhi, India

9 ²Department of Life Sciences, School of Natural Sciences, Shiv Nadar
10 University, Greater Noida, India

11

12

13 ***Correspondence:**

14 Shailja Singh

15 shailja.jnu@gmail.com

16 shailja.singh@jnu.ac.in

17

18

19

20

21 **Key words: Sphingosine, Sphingosine-1-phosphate, Sphingosine-kinase**
22 **Erythrocyte, host-parasite, metabolic-interactions**

23

24

25

26

27

28

29

30 **Abstract**

31 Sphingosine-1-phosphate (S1P) a bioactive lipid is produced in its primary
32 reservoir, erythrocytes by an enzyme Sphingosine kinase-1 (SphK-1). The
33 activation of such kinases and the subsequent S1P generation and secretion in
34 the blood serum represent a major regulator of many cellular signaling
35 cascades. Orthologue of sphingosine kinases 1 and 2 (SphK-1 and 2) that
36 catalyze the phosphorylation of sphingosine generating S1P are not present in
37 malaria parasite. The malaria parasite, *Plasmodium falciparum*, is an
38 intracellular obligatory organism that reside in the human erythrocyte during its
39 blood stage life cycle and orchestrates many metabolic interactions with host for
40 its survival. Given the regulatory role of S1P, we targeted host SphK-1 by a
41 generic pharmacological inhibitor N,N-Dimethyl-sphingosine (DMS) and
42 analyzed growth of intra-erythrocytic parasite. We found that reducing S1P
43 levels by inhibiting host SphK-1 activity led to halted parasite growth and
44 ultimately cell death. Reduced intracellular S1P levels were attributed to
45 decreased glycolysis marked by the low uptake of glucose by parasite and by
46 less production of lactate, a byproduct of glycolysis. Reduced glycolysis was
47 mediated by decrease translocation of the glycolytic enzyme, Glyceraldehyde 3-
48 phosphate dehydrogenase (GAPDH) to the cytosol of infected erythrocytes and
49 cell death. Knocking down of erythrocyte SphK-1 is not lethal to the host and
50 being a host encoded enzyme, targeting it with safe and specific drugs will not
51 lead to the problem of resistance; thus, SphK-1 represents a potent target for the
52 development of therapeutics against intra-erythrocytic *P. falciparum*.

53

54 **Author Summary**

55 Erythrocytes membrane enzyme Sphingosine kinase-1 (SphK-1) produces
56 Sphingosine-1-phosphate (S1P) a bioactive lipid by phosphorylation of
57 Sphingosine (Sph). S1P generated by activation of SphK is prosurvival signal
58 and regulate cell growth. The malaria parasite, *Plasmodium falciparum*, is an
59 intracellular obligatory pathogen that reside in erythrocyte during its blood stage
60 life cycle and orchestrates many metabolic interactions with its host
61 erythrocytes for survival. Orthologue of SphK-1/ 2 are not present in malaria
62 parasite, therefore treatment with SphK inhibitor targeted host SphK-1 and led
63 to reduced S1P level. The reduction in host S1P led to halted parasite growth
64 and cell death. Furthermore, reduced erythrocyte S1P levels led to decreased
65 glycolysis marked by the low uptake of glucose by parasite and by less
66 production of lactate. Erythrocyte SphK-1 being a host encoded enzyme, is
67 resistance safe and represents a potent target for the development of
68 therapeutics against intra-erythrocytic *P. falciparum*.

69

70

71

72

73

74

75

76

77

78

79 **Introduction**

80 An estimate of 219 million malaria cases and 435,000 related deaths were
81 reported in 2017 worldwide according to World Health Organization[1]. The
82 decrease in efficiency of current anti-malarial agents including artemisinin,
83 quinine, chloroquine, piperaquine, mefloquine and their derivatives in malaria
84 affected regions of the world has significantly increased the cost and complexity
85 of curing malaria[2][3][4]. The limited number of available anti-malarial drugs
86 and parasitic resistance to almost every available chemical therapy continues to
87 spur the search for novel approaches. The next generation of anti-malarials are
88 in pipeline and holds a great promise as they target novel parasite encoded
89 enzymes and molecular pathways[5][6]. However, since these drugs target
90 molecules that are under genetic control of the parasite, resistance against them
91 can be developed in the long run[7][8]. To deal with the nuisance of drug
92 resistance, targeting host encoded proteins that are indispensable for parasite
93 growth and survival would be an ideal situation. Since, the chances of
94 development of resistance against non-parasite targets are very bleak, host
95 targeted drug development will be a classical addition to the field of drug
96 discovery in malaria.

97 *P. falciparum* being an intracellular obligatory parasite exploits the host's
98 resources and pathways for its survival and growth. For example, parasite feeds
99 on erythrocytic hemoglobin content during the asexual blood stage
100 development. The breakdown of hemoglobin provides amino acids for its
101 growth and maturation[9]. Another important example is the metabolic pathway
102 of glycolysis. It is well known that the parasite infected erythrocytes utilize
103 glucose at a much higher rate than the normal parasite uninfected
104 erythrocytes[10][11]. During the intra-erythrocytic growth phase, *Plasmodium*
105 lacks a functional tricarboxylic acid (TCA) cycle (also known as Krebs cycle)

106 and is therefore, dependent on glycolysis for its energy requirements[12]. For
107 glycolysis, the parasite makes use of pre-existing pools of host glucose as well
108 as imports it by expressing glucose transporters on the surface of the host
109 erythrocytes[13]. The parasite's sole dependence on glycolysis for energy needs
110 makes it a potential target for anti-malarial chemotherapies. However, the
111 regulation of glycolysis by parasites in infected erythrocytes is not very
112 clear[14]:[15]:[16].

113 A recent study demonstrates that intracellular S1P facilitates glycolysis in
114 erythrocytes in response to hypoxia[17]. This biolipid is involved in various
115 other biological processes including immune response[18], bone marrow cells
116 trafficking [19], vascular integrity[20], cell survival and proliferation[21].
117 Given the diverse roles of S1P, various cell types have been identified as
118 production and store house of S1P including erythrocytes, endothelial cells,
119 thrombocytes, mast cells, and macrophages[22]:[23]. However, erythrocytes
120 have been considered as the main repository for S1P in the blood
121 plasma[22]:[24]. Several reasons have been held responsible for the elevated
122 S1P content in these cells including high sphingosine kinase (SphK) activity,
123 lack of S1P degrading enzymes (S1P lyase and S1P phosphohydrolase) and its
124 capability to import sphingosine from extracellular environment[25]:[26].
125 Surprisingly, the role of multi-faceted S1P in erythrocytes and what affect it
126 exerts on the physiology of the cells remains an unexplored mystery. S1P is
127 produced through hydrolysis of sphingomyelin to ceramide by
128 sphingomyelinases, followed by sphingosine synthesis from ceramide via the
129 action of cermidases, and finally phosphorylation of sphingosine via
130 sphingosine kinases (SphK) produces S1P[27]. S1P is basically a
131 phosphorylated product of sphingosine produced by kinases, sphingosine
132 kinase-1 and -2 (SphK-1 and SphK-2)[28]. While SphK-1 is localized to the

133 cytosol, SphK-2 resides in the nucleus[29][30]. Erythrocytes harbor only SphK-
134 1 which is the main enzyme responsible for the production of S1P in
135 them[22][24]. Phosphorylation of host SphK-1 acts as a key regulating factor
136 for its activity. SphK-1 selectively binds to phosphatidylserine in the membrane
137 and phosphorylation at serine 225 is essential for its increased selective
138 membrane binding capability[28]. Intracellular erythrocytic S1P binds to
139 deoxygenated-hemoglobin, translocates to the membrane and mediates the
140 release of the glycolytic enzyme, GAPDH, which in turn regulates the
141 erythrocytic glycolysis pathway[17]. Apart from being synthesized within the
142 erythrocytes, S1P gets secreted out in the blood plasma via a specific S1P
143 transporter major facilitator superfamily transporter (Mfsd2b)[31].

144 With this background, we aimed to study the role of host SphK-1 in regulation
145 of parasite growth inside the host erythrocytes. We demonstrated inhibition of
146 host SphK-1 by N,N-Dimethylsphingosine (DMS) lowered S1P levels in the
147 host. The Inhibition of host SphK-1 led to the reduction in glycolysis and cell
148 death of parasite. The Inhibition of SphK-1 was found to be associated with
149 reduction in cytosolic presence of glycolytic enzyme GAPDH. Glycolysis in
150 normal erythrocytes is mainly regulated by an essential cytosolic enzyme,
151 GAPDH, which remains bound to the membrane unless required during
152 glycolysis[32]. Thus, reduction of cytosolic GAPDH leads to lowered activity in
153 parasite-infected erythrocytes can be an explanation for parasite death. Since
154 deletion of host SphK-1 does not have any adverse effect on host, we advocate
155 the targeting of host SphK to kill parasite for the development of potent anti-
156 malarial drugs. Also, since it is a host-encoded enzyme, the possibility of the
157 resistance development by the parasites is diminished.

158 **Materials and methods**

159 **Cultivation of *P. falciparum*–infected erythrocytes**

160 *P. falciparum* 3D7 strain was cultured in RPMI 1640 (Invitrogen, Carlsbad, CA,
161 USA) supplemented with 27.2 mg/L hypoxanthine (Sigma-Aldrich, St. Louis,
162 MO, USA), 2 gm/L sodium bicarbonate (Sigma-Aldrich, St. Louis, MO, USA)
163 and 0.5 gm/L AlbuMax I (Gibco, Grand Island, NY, USA) using O+ human
164 erythrocytes, under mixed gas environment (5% O₂, 5% CO₂ and 90% N₂) as
165 described previously[33]. For the assessment of half-maximal drug
166 concentration for inhibition of malaria survival (IC₅₀) values, synchronized *P.*
167 *falciparum* infected erythrocyte cultures were used at late-ring or early
168 trophozoite stage (18-24 hours post infection (hpi)) at a parasitemia of 1%.
169 Where indicated, cultures were treated with the DMS inhibitor (Sigma-Aldrich,
170 St. Louis, MO, USA) at concentrations ranging from 0 to 40 μM. Untreated
171 controls were cultured in parallel under the same conditions and processed
172 identically. To assess total parasitemia, cultures were collected at the indicated
173 times and freeze-thawed. The lysates were processed for SYBR-green staining
174 (Thermo Fisher Scientific, Waltham, Massachusetts, US). Briefly, equal
175 volumes of lysis buffer containing 20 mM tris (pH 7.5), 5 mM EDTA, 0.008%
176 saponin (w/v), and 0.08% triton X-100 (v/v) was added to the lysed parasites
177 and incubated for 3 hours at 37°C with 1X SYBR-green dye. Fluorescence after
178 the SYBR-green assay was recorded in a multimode plate reader (BioRad) at
179 an excitation and emission wavelength of 485 nm and 530 nm, respectively.
180 Percent growth inhibition was calculated using the following formula: %
181 Growth Inhibition = $\{(Control - Treated) / (Control) * 100\}$. The effect of DMS
182 was tested on progression of the parasites treated at ring stage and monitored till
183 different developmental asexual stages, namely, rings, trophozoites, schizonts
184 and release of merozoites from schizonts. Tightly synchronized ring stage
185 parasite cultures treated with 10 μM DMS inhibitor or solvent as control were
186 incubated for 0, 18, 34, 45 hours blood stage asexual cycle to monitor the
187 progression at each stage. Morphological analysis and counting (~3,000 cells/

188 Giemsa-stained slides in duplicate) were done at each of these stages to monitor
189 the parasite's progression.

190 **Analysis of morphological changes in infected and uninfected erythrocytes**
191 **by Scanning Electron Microscopy (SEM) after DMS treatment**

192 The infected and uninfected erythrocytes were treated with DMS (10 μ M) for a
193 period of 5 hours. Following incubation erythrocyte and infected erythrocyte
194 were washed three times in sterile PBS. The samples were then fixed by 2.5%
195 glutaraldehyde in 1X PBS (pH 7.4) with 2% formaldehyde for a period of 30
196 minutes. Post fixation, samples were rinsed thrice with 1X PBS and dehydrated
197 in absolute ethanol series (ethanolic dehydration), using a standard protocol.
198 Samples were then completely dried, coated with gold, and observed under the
199 scanning electron microscope.

200 **Extraction of Lipids and Sphingosine-1-Phosphate Measurement**

201 Equal number of synchronous parasitized erythrocytes at 7-8% parasitaemia,
202 and uninfected erythrocytes both in presence and absence of DMS for a period
203 of 5 hours were used for further experiments. Collected cell pellets and
204 supernatant were employed for lipid extraction as reported previously [34].
205 Pellets were resuspended in 100 μ l H₂O and transferred to 900 μ l methanol.
206 Whereas, for quantification of S1P in supernatant, 1:15 ratio of methanol was
207 used. After vortexing and centrifugation at 10,000 $\times g$ for 5 minutes at RT,
208 methanol extracts were removed to a new glass tube. After evaporation by N₂,
209 dried lipids were resuspended in 200 μ l methanol. Extracted lipid samples were
210 subjected to liquid-chromatography mass-spectrometry (LC/MS) analysis. We
211 used a Waters Acquity H-Class UPLC-system (Waters, Milford, MA, USA).
212 Chromatographic separation was achieved on an Acquity BEH C18, 1.7 μ m,
213 75 \times 2.1 mm column (Waters, Manchester, UK). Mass spectrometry was
214 performed in negative electrospray mode using a high-resolution mass

215 spectrometer synapt G2 S HDMS (Waters, Manchester, UK) with a TOF-
216 detector with linear dynamic range of at least 5000:1. The mass spectra were
217 acquired over the range of 100–1000 Da with a spectral acquisition rate of
218 0.1 seconds per spectrum.

219 For S1P measurement by enzyme-linked immunosorbent assay (ELISA)
220 (MyBioSource, San Diego, USA) method, parasite infected and uninfected
221 erythrocytes were treated with 10 μ M DMS for 5 hours at 37°C. Collected
222 supernatant was used to measure extracellular S1P, whereas, the lysed
223 erythrocytes were used to measure intracellular S1P level. The samples were
224 added to the micro ELISA plate wells separately, pre-coated with S1P-specific
225 antibody for 90 minutes at 37°C followed by probing with a biotinylated
226 detection antibody specific to human S1P and incubation for 1 hour at 37°C.
227 After washing, Avidin-horseradish peroxidase (HRP) conjugate was added
228 successively to each microplate well and incubated for 30 minutes at 37°C. The
229 wells were washed to remove the unbound components followed by addition of
230 substrate solution to each well. Only those wells that contained S1P,
231 biotinylated detection antibody and Avidin-HRP conjugate appeared blue in
232 color. The enzyme-substrate reaction was terminated by addition of stop
233 solution turning the reaction color to yellow. The optical density (O.D.)
234 proportional to the S1P level was measured spectrophotometrically at a
235 wavelength of 450 nm.

236

237 **Fluorescence microscopy for uptake of NBD-Sphingosine in infected** 238 **erythrocyte.**

239 Washed infected erythrocyte (1×10^8 /mL) were incubated with 1 μ M N,N
240 Dimethyl sphingosine (Sigma Aldrich) or 1 μ M omega (7-nitro-2-1, 3-
241 benzoxadiazol-4-yl)(2S,3R,4E)-2-amino octadec-4- ene-1,3-diol (NBD–

242 sphingosine; Avanti Polar Lipids) for 15 min at 37 °C. The infected
243 erythrocytes were pelleted at 550 ×g for 5 min and resuspended in fresh
244 incomplete RPMI media. Approximately 100 µL of the samples was placed
245 onto a glass bottom petri dish. The cells were then allowed to settle at RT for 5
246 min and were viewed using a confocal Nikon Ti2 microscope equipped with a
247 100× oil objective (Melville, NY). Digital images were captured. Further,
248 images were processed via NIS-Elements software.

249

250 **Immunofluorescence assay and immunoblotting for SphK-1 and GAPDH** 251 **in erythrocytes**

252 For immunofluorescence assays, thin smears of schizont or mixed stage
253 parasites treated or untreated with DMS were made on glass slides, air dried and
254 fixed with methanol (ice cold) for 30 minutes at -20°C. Smears were blocked
255 with 3% (w/v) bovine serum albumin (BSA) in phosphate buffer saline (PBS)
256 blocking buffer (pH 7.4) for 30 minutes at room temperature (RT). Slides were
257 probed with anti-SphK-1 (Invitrogen, Carlsbad, CA, USA, 1:1000) rabbit and
258 anti-GAPDH (Invitrogen, Carlsbad, CA, USA, 1:500) mouse antibodies in
259 blocking buffer at RT for 1 hour. After washing, slides were incubated with
260 Alexa Fluor 594 conjugated goat anti-rabbit IgG (Molecular Probes, USA,
261 1:500) and Alexa Fluor 488 conjugated goat anti-mouse IgG (Molecular Probes,
262 USA, 1:500) at RT for 1 hour. After washing, the slides were mounted in
263 ProLong Gold antifade reagent (Invitrogen, Carlsbad, CA, USA), viewed on a
264 Nikon A1-R confocal microscope and Olympus confocal microscopy. Further,
265 images were processed via NIS-Elements software.

266 **Immunoblotting for SphK-1 and GAPDH in erythrocytes**

267 Parasite infected and uninfected erythrocytes in the presence or absence of
268 DMS were lysed by freeze-thawing in 10 volumes of 5 mmol/L cold phosphate
269 buffer (pH 8.0) with 1X protease inhibitor cocktail (PIC), vortexed and
270 erythrocyte membrane pellets were separated from cytosolic fraction by
271 centrifugation at 20,000 $\times g$ for 20 minutes at 4°C. The fractionated pellets were
272 washed ten times with phosphate buffer to obtain ghost erythrocytes. Total cell
273 pellet of parasite infected and uninfected erythrocytes were re-suspended in
274 RIPA buffer [100 mM phosphate buffer pH 7.2, 150 mM NaCl, 1% NP-40,
275 0.5% sodium deoxycholate, 0.1% SDS, 50 mM EDTA and 1X PIC. Equal
276 amounts of each sample were boiled with 2X Laemmli buffer, separated on a
277 10% polyacrylamide gel, transferred onto the PVDF membranes (Millipore)
278 followed by blocking with 5% skim milk blocking buffer for 1 hour at 4°C.
279 After washing, blots were incubated for 1 hour with anti-SphK-1 (1:3000), anti-
280 Phospho-SphK-1 (Ser225) (Invitrogen, Carlsbad, CA, USA, 1:1000) rabbit and
281 anti-GAPDH (Invitrogen, Carlsbad, CA, USA, 1:10,000) mouse antibodies in
282 blocking buffer. Later, the blots were washed and incubated for 1 hour with
283 appropriate secondary antibodies anti-rabbit and anti-mouse (1:10,000)
284 conjugated to HRP. Immunoblotted proteins were visualized by using the
285 Clarity Western ECL substrate (Bio-Rad).

286 **Glycolysis estimation by lactate level measurement and glucose uptake**

287 Glycolysis estimation was performed using lactate assay kit (Sigma-Aldrich, St.
288 Louis, MO, USA). Parasite infected and uninfected erythrocytes were
289 resuspended in cRPMI containing 10 μM DMS and incubated for 3 hours at
290 37°C. The supernatant was separated by centrifugation at 5000 $\times g$ for 10
291 minutes at RT and lactate levels were measured in supernatant and lysed
292 erythrocytes according to the manufacturer's protocol. Glucose uptake into the
293 parasites was quantified with 2-(*N*-(7 Nitrobenz-2-oxa-1, 3-diazol-4-yl)

294 Amino)-2-Deoxyglucose (2-NBDG) (Sigma-Aldrich, St. Louis, MO, USA)
295 via fluorescence labelling and flow cytometry. 2-NBDG is a fluorescent D-
296 glucose derivative and acts as a tracer. Synchronized trophozoite stage parasites
297 were treated with 10 μ M DMS and incubated for 3 hours at 37°C. The parasite
298 medium was replaced with RPMI without glucose supplemented with 0.3 mM
299 2-NBDG followed by incubation for 20 minutes at 37°C to allow uptake of the
300 glucose analogue. Cells were viewed on a Nikon A1-R confocal microscope
301 (Nikon, Tokyo, Japan) and further, images were processed via NIS-Elements
302 software. For flow cytometry, analysis was done on BD LSR Fortessa flow
303 (Franklin Lakes, NJ) and FlowJo software.

304 **Statistical Analysis**

305 The data for all the assays are expressed as the mean \pm standard deviation (SD)
306 of three independent experiments done in triplicates.

307 **RESULTS**

308 **Inhibition of host SphK-1 activity by specific inhibitor DMS decreases both** 309 **intracellular and extracellular S1P levels**

310 Physiologically, the main reservoir of circulating S1P is erythrocytes, which are
311 rich in SphK-1 while devoid of S1P lyase and sphingolipid transporter 2
312 (SPNS2)[25][26]. Hence, modulation of SphK-1 level could mediate change in
313 the levels of circulating or intracellular S1P concentration. Therefore, we
314 determined the level of SphK-1 in parasite infected and uninfected erythrocytes
315 by immunolabelling and immunoblotting. For immunolabelling, mixed stage
316 parasites were probed with anti-SphK-1 antibody. Significant reduction in
317 SphK-1 levels was found after treatment with DMS in parasite infected
318 erythrocytes as compared to control by two different technique. (**Fig. 1a**). To
319 further understand, if host Sphk-1 activity might be governed by

320 phosphorylation, we have evaluated the phosphorylation status of host SphK-1
321 in presence of its specific inhibitor (DMS), by probing lysate of infected
322 erythrocytes with specific anti-SphK-1 and Phospho-SphK-1 (Ser225)
323 antibodies. Whereas, GAPDH was used as a loading control. In line with the
324 previous result, host SphK-1 level was found to be reduced in parasite infected
325 erythrocytes and uninfected erythrocyte treated with DMS as compared to the
326 untreated (**Fig. 1b**). Moreover, the phosphorylated form of host SphK-1
327 (pSphK-1) was significantly reduced in parasite infected erythrocytes and
328 uninfected erythrocyte following DMS treatment. The band intensities were
329 quantified to confirm the relative changes in both level of SphK-1 and
330 phosphorylation status (**Fig. 1b**).

331 Similar results were obtained in a study done parallelly wherein, host SphK-1
332 level and activity was found to be regulated upon parasite infection to human
333 erythrocytes (manuscript in review with Frontiers). Further, to determine
334 whether host SphK-1 inhibition during parasite infection poses any alteration in
335 S1P levels, we detected the relative levels of S1P in intracellular (**IC**) and
336 extracellular (**EC**) milieu of the erythrocytes through LC/MS analysis and
337 ELISA based kit. Lipid extracts were prepared from *P. falciparum* infected
338 and/or uninfected erythrocytes in the presence or absence of 10 μ M DMS and
339 samples were then subjected to LC/MS analysis[34]. A characteristic peak at
340 position \sim 378.16 in MS spectra was detected for S1P in all the experiments
341 (**Supplementary Figure 1, 2 (A-H)**). Interestingly, the S1P level in DMS-
342 treated infected erythrocytes was almost non-detectable, while the untreated
343 infected erythrocytes demonstrated drastic reduction in S1P levels in both in IC
344 and EC microenvironments. While DMS-treated healthy erythrocytes showed
345 significant reduction in S1P levels from both IC and EC (**Supplementary**
346 **Figure 1**). In order to validate the regulation of S1P levels by DMS, ELISA-
347 based quantification was performed. The findings revealed significant down

348 regulation in S1P levels in DMS-treated infected erythrocytes, as compared to
349 untreated infected erythrocytes. Whereas, DMS treatment led to ~50% reduction
350 in both EC and IC profiles of healthy erythrocytes, when compared to untreated
351 healthy controls (**Fig. 1c**). These results implicated reduced SphK-1 activity in
352 infected erythrocytes congruent to the effect observed in the uninfected cells on
353 DMS treatment.

354 Further, we examined whether DMS affect the uptake of NBD-sphingosine or
355 not. For this the infected erythrocyte were incubated with NBD-sphingosine,
356 when NBD-sphingosine added to erythrocyte it incorporated on erythrocyte
357 membrane and get phosphorylated by SPHK-1 into NBD-S1P. phosphorylate by
358 SphK-1 and convert into NBD sphingosine 1 phosphate.[35] The result shows
359 that incubation of infected erythrocyte with NBD-sphingosine it get
360 incorporated into the erythrocyte membrane and parasite and shows
361 fluorescence which suggest the uptake of NBD sphingosine. To further
362 investigate whether the infected RBCs in presence of DMS shows the same
363 phenomenon we incubate the infected RBCs with NBD-sphingosine and DMS.
364 After treatment incubation was done for 15min at 37 and we found that in
365 treated sample NBD-sphingosine get less incorporated in parasite as well as on
366 erythrocyte membrane as compared to the control one. (**Fig. 1d**).

367 This data suggests that inhibition of Sphk-1 by DMS causes less uptake of
368 NBP-sphingosine as well as less production of S1P which is supported via LC-
369 MS profiling

370

371 **Inhibition of erythrocytic SphK-1 triggers parasite death**

372 To decipher the link between host SphK1 activity and parasite growth, we have
373 elucidated the effect of DMS on synchronized parasite cultures at ring stage.
374 DMS treatment was done in an increasing manner (0, 5, 10, 20, 30 and 40 μ M)

375 for 48 hours. After completion of one asexual life cycle of the parasite, SYBR-
376 green was added for assessing the percentage inhibition by DMS. The data
377 revealed a moderate to potent anti-malarial activity of DMS with a significant
378 reduction in the parasite load, with IC₅₀ value attended at 14 μM (**Fig. 2a**). To
379 examine its impact on stage specific inhibition of parasite progression, highly
380 synchronized ring stage parasites were treated with 10 μM DMS and their
381 development were monitored at different time intervals (0, 18, 34, 45 hpi) by
382 preparing thin blood smears of the treated and untreated infected erythrocytes.
383 As observed in the blood smears, DMS drastically affected progression of the
384 parasite from rings to trophozoites, stalling the parasite progress at the ring
385 stage as compared to the untreated parasite infected control. Halt in the parasite
386 growth could be accounted to the formation of ‘pyknotic body’ after 36 hours of
387 the treatment (**Fig. 2b**). This progression arrest coincided with a significant drop
388 in the S1P levels of the erythrocytes after DMS treatment. These findings
389 strongly support the hypothesis, which suggested that SphK-1 mediated
390 production of S1P plays an important role in *Plasmodium* growth and
391 development in the erythrocytes. Further, to ascertain whether the host SphK-1
392 inhibition mediated retardation of parasite growth and progression in
393 independent of DMS-induced topological aberration in host membrane, we have
394 performed SEM-based imaging of both infected and uninfected erythrocytes in
395 presence of DMS. The SEM micrographs hardly show any significant changes
396 in infected erythrocytes, following DMS treatment as compared to the
397 respective untreated control (**Fig. 2c**). Similar observation could also be inferred
398 from the experiments involving uninfected erythrocytes treated with DMS (**Fig.**
399 **2c**).

400 **Inhibition of erythrocyte SphK-1 results in decrease in lactate production**

401 The intra-erythrocytic stages of *P. falciparum* lack a functional citric acid cycle
402 and is largely reliant on glycolysis to fulfill its very substantial energy
403 requirements[36][37]. Erythrocytes infected with mature trophozoite stage
404 parasites consume glucose up to two folds of magnitude faster than uninfected
405 erythrocytes, eventually converting it to lactic acid[10][11][38]. To dissect this
406 mechanism of SphK-1 dependent growth progression in parasite infected
407 erythrocytes, and its link to glycolysis, we estimated the amount of lactate
408 formation, an indicator of glycolytic process, in both infected and uninfected
409 erythrocytes in presence of 10 μ M DMS for 3 hours. The findings suggested a
410 prominent reduction in lactate production in DMS-treated infected and
411 uninfected erythrocytes, as compared to respective untreated controls (**Fig. 3a**).
412 Interestingly, parasite stage-specific estimation of lactate levels during intra
413 erythrocytic cycle, represented predominant decrease in lactate production, as
414 clearly evident in rings, trophozoites and schizonts (**Fig. 3b**), following
415 treatment with 10 μ M of DMS for 3 hour. These data depict that; lowering of
416 S1P levels by DMS-based inhibition of host SphK1 can lead to compromised
417 glycolysis, which is manifested as reduced lactate levels in intra-erythrocytic
418 cycle of *P. falciparum*.

419 To gain further insight, whether the observed metabolic alterations after
420 inhibitor treatment were mediated specifically through erythrocytes or it directly
421 impacted the parasite, we have elucidated the changes in lactate levels in host-
422 free parasite isolated by saponin lysis, in response to the inhibitor. To
423 determine the intrinsic lactate level of the trophozoite stage along with the
424 saponin lysed host-free parasites were treated with the inhibitor for 2 hours.
425 Interestingly, the lactate levels were found to be lowered as compared to their
426 respective untreated controls except in the case of saponin lysed parasites
427 wherein, there was no significant difference in the lactate levels of DMS treated

428 and untreated parasites could be detected (**Fig. 3c**). Lowering of lactate levels
429 could be accountable to either down regulated glycolysis rate and/or reduced
430 glucose uptake in trophozoite infected and uninfected erythrocytes. However,
431 saponin lysed/host-free DMS treated trophozoites demonstrated negligible
432 difference in the lactate levels as compared to the untreated control, suggesting
433 erythrocytes as the mediator of S1P-dependent glycolysis not the parasite (**Fig.**
434 **3c**). Altogether, these readouts suggested that host SphK-1 contributes to the
435 regulation of glycolysis and its effect on parasite growth is mediated solely
436 through the erythrocyte.

437 **Abrogated S1P synthesis results in reduced glucose uptake**

438 Further, we investigated the role of S1P in glucose uptake and glycolysis, as
439 erythrocytes are solely dependent on glycolysis to meet their energy
440 requirements. Towards this, we measured the glucose uptake in parasite-
441 infected erythrocytes via fluorescence labelling and fluorescence-activated cell
442 sorting (FACS) using a non-metabolizable glucose analog, 2-NBDG, which is
443 fluorescently tagged. 2-NBDG accumulates inside the cells by entering through
444 the glucose transporters but it does not enter into the glycolysis
445 pathway[38][39][40]. Parasite infected erythrocytes were pre-incubated with
446 DMS or solvent control for 3 hours at 37°C. The cells were then incubated with
447 fluorescently labeled 2-NBDG and its uptake was measured after washing the
448 cells with PBS using confocal microscopy and flow cytometry. Live-cell
449 imaging of DMS-treated infected erythrocytes represented drastic reduction in
450 glucose uptake, as represented by diminished green fluorescence indicating
451 lower uptake of 2-NBDG. While, the untreated infected erythrocytes displayed
452 prominent green fluorescence suggesting healthy uptake of glucose analogues
453 (**Fig. 4a**). The fluorescence intensities were plotted using Image J for the
454 treated and untreated cells indicating the same (**Fig. 4a**). To confirm whether

455 the impaired uptake of glucose analogue in DMS-treated infected erythrocytes
456 was due to dysregulated glycolysis but not compromised cell viability, we used
457 a strategy using dual dye-based assay. Regarding this, we have used Syto9 in
458 combination with Propidium Iodide (Thermo Fisher Scientific, Waltham,
459 Massachusetts, US) to delineate viability in DMS-treated infected erythrocytes.
460 The finding revealed that the viability was uncompromised in DMS-treated
461 infected erythrocytes with significant reduction in 2-NBDG uptake, suggesting
462 the impairment in glucose uptake was mainly due to altered S1P level following
463 host SphK-1 inhibition by DMS. Further, flow cytometry analysis of 2-NBDG
464 uptake in DMS-treated infected erythrocytes demonstrated a 10-fold shift in
465 fluorescence intensity indicating enhanced uptake of 2-NBDG, whereas, the
466 untreated infected erythrocytes showed severe depletion in 2-NBDG uptake, as
467 shown by diminished intensity peak in representative histogram (**Fig. 4b**).
468 These results suggested that the uptake of glucose analogue, a signature of
469 healthy glycolysis, was strongly repressed by the host SphK-1 inhibition as
470 compared to their respective controls.

471 **Inhibition of erythrocyte SphK-1 leads to change in translocation of**
472 **glycolytic enzyme GAPDH from membrane-to-cytosol**

473 Intracellular S1P in erythrocytes has been known to release membrane-bound
474 GAPDH, a glycolytic enzyme to cytosol in response to hypoxia[17]. Since, host
475 SphK-1 inhibition led to depletion in S1P levels in infected erythrocytes, we
476 assumed translocation of GAPDH from membrane to cytosol might be also be
477 hampered in DMS-treated infected erythrocytes. To validate the same, we
478 checked the levels of GAPDH in cytosolic and membrane fractions of parasite
479 infected and uninfected erythrocytes. The GAPDH level was detected by
480 immunoblotting and immunolabelling. The total cell lysate was used as a
481 control. After DMS treatment, both the membrane and cytosolic fractions were

482 separated for probing with anti-GAPDH mouse antibody. As expected, DMS
483 treatment restricted the translocation of GAPDH to the erythrocyte membrane,
484 as evident in immunoblot and its respective band intensities in both membrane
485 and cytosolic fractions (**Fig. 5a**). These findings confirmed low release of
486 GAPDH to the cytosol due to altered glycolysis in DMS-treated infected
487 erythrocytes. Further, we visualized the localization of GAPDH in the cells by
488 immunolabelling using confocal imaging. After DMS treatment, GAPDH was
489 mainly restricted to the erythrocytic membrane rather than translocating to the
490 cytosol, suggesting decreased glycolysis, which can be corroborated to our
491 previous findings (**Fig. 5b**). Collectively, these results suggested low S1P levels
492 in DMS-treated infected erythrocytes can lead to aborted glycolysis.

493 **Discussion**

494 It is noteworthy that, circulating erythrocytes demonstrate high storage of S1P,
495 a crucial signaling biolipid, as compared to other peripheral tissues, especially
496 due to lack of S1P degrading enzyme, Sphingosine 1 phosphate lyase
497 (SPL)[17]. However, the erythrocytes do express S1P transporter Mfsd2b[31]
498 and the concentration gradient of S1P from circulating erythrocytes to
499 peripheral tissues governs several critical physiological processes, including
500 vascular integrity, trafficking of lymphocytes and bone homeostasis
501 *etc*[41][20][42].

502 S1P also play as a rheostat for maintaining balance between cytoysis and
503 apoptosis[43]. In addition, the SphK-1/S1P signaling nexus contributes to the
504 development and progression of various diseases including, Huntington's
505 disease [44] and ulcerative colitis[45] *etc*. Thus, modulation of SphK-1 enzyme
506 and its products have become the prime target in order to reduce the disease
507 severity[46][47]. S1P is catalyzed by two isoforms of Sphingosine kinase,
508 SphK (isoforms SphK-1 and SphK-2), and can turn on various cellular

509 processes by activating a family of G protein-coupled receptors, sphingosine-1-
510 phosphate receptor 1-5 (S1P₁₋₅)[48].

511 Accumulating body of evidences reveal strong role of deregulated S1P
512 metabolism in parasite-born diseases, including trypanosomiasis, leishmaniasis
513 and cerebral malaria[49][50][51]. However, studies involving host-SphK1
514 mediated manipulation of parasite growth and progression are still at their
515 infancy and unraveling the same would provide a breakthrough to present
516 alternative targets for the drug therapies. With this perspective, we have
517 delineated the possible role of host-SphK1 activity on growth and progression
518 of *P. falciparum*, the causative agent of malaria, one of the deadly parasitic
519 diseases.

520 To achieve this, we targeted host SphK-1 activity by using a specific inhibitor
521 DMS, which completely depleted the S1P levels in both IC and EC of infected
522 erythrocytes, leading to stalled the parasitic growth and progression with
523 formation of ‘pyknotic bodies’ (**Fig. 1, 2**). To negate the possibility of DMS-
524 enforced topological alterations in infected erythrocytes as the basis of aborted
525 parasite growth and invasion, we have performed SEM-based analysis of both
526 uninfected and infected erythrocyte membranes after DMS treatment. To
527 emphasize, there was no significant changes could be identified in membrane
528 structures of infected erythrocytes even after DMS treatment (**Fig. 2c**). Similar
529 inference was drawn from the experiment involving uninfected erythrocytes
530 with DMS (**Fig. 2c**). Since erythrocytes mainly harbor SphK-1, but no S1P
531 receptor for its innate signaling, we hypothesized that inhibiting host-SphK1,
532 might be attenuating the host-S1P dependent parasite survival mechanism as
533 well. During *Plasmodium* infection, erythrocytes demonstrate 6-fold increase in
534 phospholipids (PL), along with a sharp rise in glycolytic flux, with glucose
535 uptake upto 50 folds, predominant in metabolically progressive stages such as

536 (trophozoite and schizont)[52][53][54] suggesting host-dependency of the
537 parasite for fulfilling its metabolic needs[55].

538 To understand, whether inhibition of host-SphK1 during infection might block
539 glycolysis in metabolically active stages of *P. falciparum*, mainly in trophozoite
540 and schizont; we have estimated the levels of lactate, a signature metabolite in
541 the same following DMS treatment. The results depict, drastic switch of
542 metabolically active stage of parasites to metabolically dormant state, leading to
543 parasite growth retardation (**Fig. 2, 3**). This data strongly advocated the role of
544 host-SphK1 in regulation of glycolysis-dependent growth and progression of
545 parasites. Further, to confirm the hypothesis, which suggested that altered
546 glycolysis of intra-erythrocytic cycles is mediated specifically through
547 erythrocytes not via the parasites; we also estimated the lactate levels in DMS-
548 treated saponized/host-free parasites, as a proof-of-concept. The observation
549 clearly ruled out the involvement of parasite-mediated glycolysis, as no change
550 in lactate levels could be detected in host-free parasites (**Fig. 3**). To elucidate
551 the impact of host SphK-1 inhibition on glucose uptake, during intra-
552 erythrocytic development, we have measured the live uptake of glucose using a
553 fluorescent-labeled glucose analogue (2-NBDG). The results presented
554 abrogated glucose uptake in DMS-treated infected erythrocytes, imposing a
555 direct role of host-SphK-1 in regulation of glycolysis (**Fig. 4**).

556 According to a recent study by K Sun et al., SphK-1 activity gets elevated in
557 erythrocytes under hypoxic conditions, leading to enhanced S1P level and
558 thereby, increasing its binding to deoxygenated hemoglobin (deoxy-Hb).
559 Subsequently, this facilitates deoxy-Hb anchorage to the membrane, leading to
560 more release of membrane-bound GAPDH to the cytosol which then increases
561 the erythrocytic glycolysis[17]. To further evaluate, whether abolishing the
562 host-SphK-1 activity in DMS-treated infected erythrocytes, would dysregulate

563 the GAPDH level, we have evaluated the level of GAPDH both in membrane
564 and cytosolic fractions. The findings unraveled reduced translocation of
565 GAPDH from membrane-to-cytosol in DMS-treated infected erythrocytes, as
566 evident from altered localized level of GAPDH, in both immunoblot and
567 confocal micrographs (**Fig. 5**). To summarize, our study highlights two
568 important findings; firstly, the inhibition of host SphK-1 activity can abrogate
569 intra-erythrocytic growth and progression of *P. falciparum*, and secondly,
570 diminished S1P levels can lead to host-mediated altered glycolysis resulting in
571 growth retardation of parasites (**Fig. 6**). Overall, this study introduces SphK-
572 1/S1P signaling nexus in erythrocytes as the alternate pathway for *P. falciparum*
573 survival. Since, knocking down of host SphK-1 is not lethal, thus targeting the
574 same would eliminate the problem of resistance. Conceivably, further
575 elucidation of SphK-1/S1P signaling pathways during parasite infection, might
576 aid in developing novel anti-malarial chemotherapeutics.

577

578 **Acknowledgments**

579 We are thankful to Advanced Instrumentation and Research Facility
580 (AIRF), Jawaharlal Nehru University (JNU), New Delhi for Central
581 Instrumentation Facility (CIF) of Special Centre for Molecular Medicine, JNU
582 for confocal microscopy, LC/MS analysis and other instruments facilities.
583 This work was supported by Bio-Scientist Award and Innovative Young
584 Biotechnologist Award (IYBA) from the Department of Biotechnology,
585 Ministry of Science and Technology, Government of India (DBT). Shailja
586 Singh is a recipient of the National Bio scientist and IYBA Award from DBT.
587 R.K.S. is supported by CSIR-UGC fellowship. M.S. is financially supported by
588 Shiv Nadar Foundation fellowships. We acknowledge the financial support
589 from Science and Engineering Research Board (SERB, File no.

590 EMR/2016/005644), India, National Institutes of Health (NIH, Grant no.
591 U19AI089676-09), United States, Department of Science & Technology-
592 Promotion of University Research and Scientific Excellence (DST-PURSE,
593 Phase II, JNU), India. The funders had no role in study design, data collection
594 and analysis, decision to publish, or preparation of the manuscript.

595

596 **Competing interests**

597 The authors declare that they have no competing interests.

598

599 **Author Contributions**

600 SS conceived and designed the research. RKS performed research and SS,
601 RKS & SP analyzed the data. RKS and SS conducted the lipid extraction and
602 estimation experiments. MS and RKS performed microscopy experiments.
603 SS, RKS, MS & SP wrote the manuscript. SS finally edited the manuscript.

604

605 **References**

- 606 1. WHO. World malaria report 2018. Geneva:World Health Organization;
607 2018. World Malaria Report. 2018. doi:ISBN 978 92 4 1564403
- 608 2. Petersen I, Eastman R, Lanzer M. Drug-resistant malaria : Molecular
609 mechanisms and implications for public health. 2011;585: 1551–1562.
610 doi:10.1016/j.febslet.2011.04.042
- 611 3. Neill PMO, Mukhtar A, Stocks PA, Randle LE, Hindley S, Ward SA, et
612 al. Isoquine and Related Amodiaquine Analogues : A New Generation of
613 Improved 4-Aminoquinoline Antimalarials. 2003; 4933–4945.
614 doi:10.1021/jm030796n

- 615 4. Briolant S, Pelleau S, Bogreau H, Hovette P, Zettor A, Castello J, et al. In
616 vitro susceptibility to quinine and microsatellite variations of the
617 Plasmodium falciparum Na⁺/H⁺ exchanger (Pfnhe-1) gene: The absence
618 of association in clinical isolates from the Republic of Congo. *Malar J.*
619 2011; doi:10.1186/1475-2875-10-37
- 620 5. Plowe C V., Roper C, Barnwell JW, Happi CT, Joshi HH, Mbacham W, et
621 al. World Antimalarial Resistance Network (WARN) III: Molecular
622 markers for drug resistant malaria. *Malaria Journal.* 2007.
623 doi:10.1186/1475-2875-6-121
- 624 6. Nolan T. Identifying an essential interaction between malaria parasites and
625 erythrocytes unlocks the door to promising vaccine targets. *Pathog Glob*
626 *Health.* 2012; doi:10.1179/204777312x13305103762583
- 627 7. Anderson TJC, Nair S, Nkhoma S, Williams JT, Imwong M, Yi P, et al.
628 High Heritability of Malaria Parasite Clearance Rate Indicates a Genetic
629 Basis for Artemisinin Resistance in Western Cambodia. *J Infect Dis.*
630 2010; doi:10.1086/651562
- 631 8. Miotto O, Amato R, Ashley EA, Macinnis B, Almagro-Garcia J,
632 Amaratunga C, et al. Genetic architecture of artemisinin-resistant
633 Plasmodium falciparum. *Nat Genet.* 2015; doi:10.1038/ng.3189
- 634 9. Francis SE, Sullivan DJ, Goldberg and DE. HEMOGLOBIN
635 METABOLISM IN THE MALARIA PARASITE PLASMODIUM
636 FALCIPARUM . *Annu Rev Microbiol.* 2002;
637 doi:10.1146/annurev.micro.51.1.97
- 638 10. Homewood CA. Carbohydrate metabolism of malarial parasites. *Bulletin*
639 *of the World Health Organization.* 1977.

- 640 11. Olszewski KL, Llinás M. Central carbon metabolism of Plasmodium
641 parasites. *Mol Biochem Parasitol.* 2011;
642 doi:10.1016/j.molbiopara.2010.09.001
- 643 12. Ke H, Lewis IA, Morrissey JM, McLean KJ, Ganesan SM, Painter HJ, et
644 al. Genetic investigation of tricarboxylic acid metabolism during the
645 plasmodium falciparum life cycle. *Cell Rep.* 2015;
646 doi:10.1016/j.celrep.2015.03.011
- 647 13. Srivastava A, Philip N, Hughes KR, Georgiou K, MacRae JI, Barrett MP,
648 et al. Stage-Specific Changes in Plasmodium Metabolism Required for
649 Differentiation and Adaptation to Different Host and Vector
650 Environments. *PLoS Pathog.* 2016; doi:10.1371/journal.ppat.1006094
- 651 14. Velanker SS, Ray SS, Gokhale RS, Suma S, Balaram H, Balaram P, et al.
652 Triosephosphate isomerase from Plasmodium falciparum: The crystal
653 structure provides insights into antimalarial drug design. *Structure.* 1997;
654 doi:10.1016/S0969-2126(97)00230-X
- 655 15. Kim J-W, Dang C V. Multifaceted roles of glycolytic enzymes. *Trends*
656 *Biochem Sci.* 2005; doi:10.1016/j.tibs.2005.01.005
- 657 16. Verlinde CLMJ, Hannaert V, Blonski C, Willson M, Périé JJ, Fothergill-
658 Gilmore LA, et al. Glycolysis as a target for the design of new anti-
659 trypanosome drugs. *Drug Resist Updat.* 2001;
660 doi:10.1054/drup.2000.0177
- 661 17. Sun K, Zhang Y, D'Alessandro A, Nemkov T, Song A, Wu H, et al.
662 Sphingosine-1-phosphate promotes erythrocyte glycolysis and oxygen
663 release for adaptation to high-altitude hypoxia. *Nat Commun.* 2016;7: 1–
664 13. doi:10.1038/ncomms12086

- 665 18. Alvarez SE, Harikumar KB, Hait NC, Allegood J, Strub GM, Kim EY, et
666 al. Sphingosine-1-phosphate is a missing cofactor for the E3 ubiquitin
667 ligase TRAF2. *Nature*. 2010; doi:10.1038/nature09128
- 668 19. Jenne CN, Enders A, Rivera R, Watson SR, Bankovich AJ, Pereira JP, et
669 al. T-bet–dependent S1P 5 expression in NK cells promotes egress from
670 lymph nodes and bone marrow . *J Exp Med*. 2009;
671 doi:10.1084/jem.20090525
- 672 20. Camerer E, REGARD JB, Cornelissen I, Srinivasan Y, Duong DN, Palmer
673 D, et al. Sphingosine-1-phosphate in the plasma compartment regulates
674 basal and inflammation-induced vascular leak in mice. *J Clin Invest*. 2009;
- 675 21. Inniss K, Moore H. Mediation of Apoptosis and Proliferation of Human
676 Embryonic Stem Cells by Sphingosine-1-Phosphate. *Stem Cells Dev*.
677 2007; doi:10.1089/scd.2006.15.789
- 678 22. Hänel P, Andréani P, Gräler MH. Erythrocytes store and release
679 sphingosine 1-phosphate in blood. *FASEB J*. 2007;21: 1202–1209.
680 doi:10.1096/fj.06-7433com
- 681 23. Schaphorst KL, Chiang E, Jacobs KN, Zaiman A, Natarajan V, Wigley F,
682 et al. Role of sphingosine-1 phosphate in the enhancement of endothelial
683 barrier integrity by platelet-released products. *Am J Physiol Cell Mol*
684 *Physiol*. 2015; doi:10.1152/ajplung.00311.2002
- 685 24. Bode C, Sensken SC, Peest U, Beutel G, Thol F, Levkau B, et al.
686 Erythrocytes serve as a reservoir for cellular and extracellular sphingosine
687 1-phosphate. *J Cell Biochem*. 2010; doi:10.1002/jcb.22507
- 688 25. Le Stunff H, Giussani P, Maceyka M, Lépine S, Milstien S, Spiegel S.

- 689 Recycling of sphingosine is regulated by the concerted actions of
690 sphingosine-1-phosphate phosphohydrolase 1 and sphingosine kinase 2. *J*
691 *Biol Chem.* 2007; doi:10.1074/jbc.M703329200
- 692 26. Zhou J, Saba JD. Identification of the first mammalian sphingosine
693 phosphate lyase gene and its functional expression in yeast. *Biochem*
694 *Biophys Res Commun.* 1998; doi:10.1006/bbrc.1997.7993
- 695 27. Nakahara K, Ohkuni A, Kitamura T, Abe K, Naganuma T, Ohno Y, et al.
696 The Sjögren-Larsson Syndrome Gene Encodes a Hexadecenal
697 Dehydrogenase of the Sphingosine 1-Phosphate Degradation Pathway.
698 *Mol Cell.* 2012; doi:10.1016/j.molcel.2012.04.033
- 699 28. Maceyka M, Sankala H, Hait NC, Le Stunff H, Liu H, Toman R, et al.
700 SphK1 and SphK2, sphingosine kinase isoenzymes with opposing
701 functions in sphingolipid metabolism. *J Biol Chem.* 2005;
702 doi:10.1074/jbc.M502207200
- 703 29. Ding G, Sonoda H, Yu H, Kajimoto T, Goparaju SK, Jahangeer S, et al.
704 Protein kinase D-mediated phosphorylation and nuclear export of
705 sphingosine kinase S. *J Biol Chem.* 2007; doi:10.1074/jbc.M701641200
- 706 30. Hengst JA, Guilford JM, Fox TE, Wang X, Conroy EJ, Yun JK.
707 Sphingosine kinase 1 localized to the plasma membrane lipid raft
708 microdomain overcomes serum deprivation induced growth inhibition.
709 *Arch Biochem Biophys.* 2009; doi:10.1016/j.abb.2009.09.013
- 710 31. Vu TM, Ishizu AN, Foo JC, Toh XR, Zhang F, Whee DM, et al. Mfsd2b
711 is essential for the sphingosine-1-phosphate export in erythrocytes and
712 platelets. *Nature.* 2017;550: 524–528. doi:10.1038/nature24053

- 713 32. Low PS, Rathinavelu P, Harrison ML. Regulation of glycolysis via
714 reversible enzyme binding to the membrane protein, band 3. *J Biol Chem.*
715 1993;
- 716 33. Trager W, Jensen JB. Human malaria parasites in continuous culture.
717 *Science* (80-). 1976; doi:10.1126/science.781840
- 718 34. Zhao Z, Xu Y. An extremely simple method for extraction of
719 lysophospholipids and phospholipids from blood samples. *J Lipid Res.*
720 2010;51: 652–659. doi:10.1194/jlr.D001503
- 721 35. Kobayashi N, Otsuka M, Yamaguchi A, Nishi T. Fluorescence-based
722 rapid measurement of sphingosine-1-phosphate transport activity in
723 erythrocytes. *J Lipid Res.* 2016;57: 2088–2094. doi:10.1194/jlr.D071068
- 724 36. Van Niekerk DD, Penkler GP, Du Toit F, Snoep JL. Targeting glycolysis
725 in the malaria parasite *Plasmodium falciparum*. *FEBS J.* 2016;
726 doi:10.1111/febs.13615
- 727 37. van Schalkwyk DA, Priebe W, Saliba KJ. The Inhibitory Effect of 2-Halo
728 Derivatives of D-Glucose on Glycolysis and on the Proliferation of the
729 Human Malaria Parasite *Plasmodium falciparum*. *J Pharmacol Exp Ther.*
730 2008; doi:10.1124/jpet.108.141929
- 731 38. O’Neil RG, Wu L, Mullani N. Uptake of a fluorescent deoxyglucose
732 analog (2-NBDG) in tumor cells. *Mol Imaging Biol.* 2005;
733 doi:10.1007/s11307-005-0011-6
- 734 39. Zou C, Wang Y, Shen Z. 2-NBDG as a fluorescent indicator for direct
735 glucose uptake measurement. *J Biochem Biophys Methods.* 2005;
736 doi:10.1016/j.jbbm.2005.08.001

- 737 40. Nitin, Carlson AL, Muldoon T, El-Naggar AK, Gillenwater A, Richards-
738 Kortum R. Molecular imaging of glucose uptake in oral neoplasia
739 following topical application of fluorescently labeled deoxy-glucose. *Int J*
740 *Cancer*. 2009; doi:10.1002/ijc.24222
- 741 41. Pappu R, Schwab SR, Cornelissen I, Pereira JP, Regard JB, Xu Y, et al.
742 Promotion of lymphocyte egress into blood and lymph by distinct sources
743 of sphingosine-1-phosphate. *Science* (80-). 2007;
744 doi:10.1126/science.1139221
- 745 42. Ishii M, Egen JG, Klauschen F, Meier-Schellersheim M, Saeki Y, Vacher
746 J, et al. Sphingosine-1-phosphate mobilizes osteoclast precursors and
747 regulates bone homeostasis. *Nature*. 2009; doi:10.1038/nature07713
- 748 43. Sankala HM, Hait NC, Paugh SW, Shida D, Lépine S, Elmore LW, et al.
749 Involvement of sphingosine kinase 2 in p53-independent induction of p21
750 by the chemotherapeutic drug doxorubicin. *Cancer Res*. 2007;
751 doi:10.1158/0008-5472.CAN-07-2090
- 752 44. Di Pardo A, Pepe G, Castaldo S, Marracino F, Capocci L, Amico E, et al.
753 Stimulation of Sphingosine Kinase 1 (SPHK1) Is Beneficial in a
754 Huntington's Disease Pre-clinical Model. *Front Mol Neurosci*. 2019;
755 doi:10.3389/fnmol.2019.00100
- 756 45. Sun M, Du B, Shi Y, Lu Y, Zhou Y, Liu B. Combined Signature of the
757 Fecal Microbiome and Plasma Metabolome in Patients with Ulcerative
758 Colitis. *Med Sci Monit*. 2019; doi:10.12659/MSM.916009
- 759 46. Maceyka M, Harikumar KB, Milstien S, Spiegel S. Sphingosine-1-
760 phosphate signaling and its role in disease. 2013;22: 50–60.
761 doi:10.1016/j.tcb.2011.09.003.

- 762 47. Obinata H, Hla T. Sphingosine 1-phosphate and inflammation. *Int*
763 *Immunol.* 2019; doi:10.1093/intimm/dxz037
- 764 48. Pyne NJ, McNaughton M, Boomkamp S, MacRitchie N, Evangelisti C,
765 Martelli AM, et al. Role of sphingosine 1-phosphate receptors,
766 sphingosine kinases and sphingosine in cancer and inflammation.
767 *Advances in Biological Regulation.* 2016. doi:10.1016/j.jbior.2015.09.001
- 768 49. Arish M, Husein A, Ali R, Tabrez S, Naz F, Ahmad MZ, et al.
769 Sphingosine-1-phosphate signaling in *Leishmania donovani* infection in
770 macrophages. *PLoS Negl Trop Dis.* 2018;12.
771 doi:10.1371/journal.pntd.0006647
- 772 50. Dominguez MR, Ersching J, Lemos R, Machado A V., Bruna-Romero O,
773 Rodrigues MM, et al. Re-circulation of lymphocytes mediated by
774 sphingosine-1-phosphate receptor-1 contributes to resistance against
775 experimental infection with the protozoan parasite *Trypanosoma cruzi*.
776 *Vaccine.* 2012; doi:10.1016/j.vaccine.2012.02.037
- 777 51. Finney CAM, Hawkes CA, Kain DC, Dhabangi A, Musoke C, Cserti-
778 Gazdewich C, et al. S1P Is Associated with Protection in Human and
779 Experimental Cerebral Malaria. *Mol Med.* 2011;
780 doi:10.2119/molmed.2010.00214
- 781 52. Wein S, Ghezal S, Buré C, Maynadier M, Périgaud C, Vial HJ, et al.
782 Contribution of the precursors and interplay of the pathways in the
783 phospholipid metabolism of the malaria parasite. *J Lipid Res.* 2018;
784 doi:10.1194/jlr.m085589
- 785 53. Gulati S, Ekland EH, Ruggles K V., Chan RB, Jayabalasingham B, Zhou
786 B, et al. Profiling the Essential Nature of Lipid Metabolism in Asexual

787 Blood and Gametocyte Stages of *Plasmodium falciparum*. *Cell Host*
788 *Microbe*. 2015;18: 371–381. doi:10.1016/j.chom.2015.08.003

789 54. Tran PN, Brown SHJ, Rug M, Ridgway MC, Mitchell TW, Maier AG.
790 Changes in lipid composition during sexual development of the malaria
791 parasite *Plasmodium falciparum*. *Malar J*. 2016; doi:10.1186/s12936-016-
792 1130-z

793 55. Mehta M, Sonawat HM, Sharma S. Glycolysis in *Plasmodium falciparum*
794 results in modulation of host enzyme activities. *J Vector Borne Dis*. 2006;

795

796 **Figure 1. Inhibition of host SphK-1 by specific inhibitor DMS causes**
797 **decrease in SphK-1 protein level and S1P levels. a)** Confocal micrographs
798 demonstrate altered host SphK-1 level in mixed-stage parasite culture following
799 treatment with DMS (10 μ M). Bar graph denotes the differential mean
800 fluorescence intensity (MFI) denoting host SphK-1 level in infected and
801 uninfected erythrocytes following DMS treatment. **b)** Evaluation of level and
802 phosphorylation status of SphK-1 by immunoblotting. Total cell lysates probed
803 with GAPDH was used as a loading control. The graph represents fold change
804 in the band intensity in individual lanes. **c)** Bar graph depicts ELISA-based S1P
805 quantification in IC and EC microenvironments of infected and uninfected
806 erythrocytes. **d)** NBD-Sphingosine-1-phosphate is localized to membrane and
807 parasite. Infected erythrocyte were resuspended in buffer containing fatty acid-
808 free BSA (0.1% (w/v)) and incubated with DMS (10 μ M) or NBD-sphingosine
809 (1 μ M) for at least 15 min at 37 °C. The Infected erythrocytes were imaged by
810 fluorescence using a 100 \times oil objective on a Nikon Ti2 microscope.

811

812 **Figure 2. Inhibition of host SphK-1 blocks parasite growth and**
813 **progression.** A) Percentage inhibition of *P. falciparum* growth was evaluated at
814 different DMS concentrations (0-40 μ M), as presented in the bar graph. Three
815 independent experiments were performed in triplicates with 96-well plates using
816 a SYBR-green assay. The IC₅₀ value was determined as 14 μ M for the parasite
817 growth inhibition with DMS. B) Visualization of stage specific inhibition of *P.*
818 *falciparum* progression following DMS treatment was depicted by light
819 microscopic images of Giemsa stained ring, trophozoite and schizont stages. C)
820 Scanning electron micrographs of DMS-treated infected and uninfected
821 erythrocytes represented comparative morphometric analysis. Scale bars = 5 μ
822 m

823

824 **Figure 3. Inhibition of host SphK-1 results in reduction of lactate**
825 **production.** A) Quantification of lactate in EC microenvironments of
826 uninfected and infected erythrocytes treated with DMS (10 μ M), was
827 represented as changes in relative intensities. B) Evaluation of lactate levels in
828 asexual blood stages following DMS treatment, was plotted as percentage fold
829 change. C) Light microscopic images of saponized/host-free trophozoites and
830 percoll purified trophozoites were visually compared following Giemsa-
831 staining. Following identification, the purified and saponized samples were
832 further used for above experiment. Representative bar graph displayed changes
833 in lactate levels as relative intensities for trophozoites and saponized/host-free
834 parasites

835 **Figure 4. Detection of glucose uptake by parasite infected erythrocytes**
836 **upon host SphK-1 inhibition.** A) Evaluation of 2-NBDG uptake in parasite
837 infected erythrocytes following DMS treatment by live-cell imaging. Respective

838 MFI of individual infected erythrocytes were plotted against individual
839 untreated cells. **B)** Representative histograms depict changes in number of
840 FITC^{positive} population in flow cytometry analysis correlating to 2-NBDG uptake
841 following DMS treatment in infected erythrocytes.

842 **Figure 5. Host SphK-1 mediated translocation of GAPDH in parasite**
843 **infected erythrocytes. A)** Detection of localized level of GAPDH in both
844 membrane and cytosolic fractions of DMS-treated infected erythrocytes. Total
845 cell lysate was used as a loading control. Change in the level was plotted as
846 relative intensities of bands detected in different cellular fractions. **B)** Confocal
847 micrographs demonstrate GAPDH level and localization in both DMS-treated
848 and untreated infected erythrocytes.

849 **Figure 6.** In the proposed working model, life cycle of blood stage parasite is
850 shown. In normal condition, S1P bind to deoxy-Hb and facilitates binding of
851 deoxy-Hb to membrane and release of GAPDH; increased cytosolic GAPDH
852 accelerates glycolysis and generate lactate which is a by-product of glycolysis
853 and does not stall the growth of parasite. In case of DMS-mediated inhibition of
854 host SphK-1, S1P level gets reduced, leading to altered binding with deoxy-Hb.
855 Thus, it does not facilitate GAPDH to cytosol due to which glycolysis is
856 suppressed leading to retarded parasite growth.

857

858

859

860

861

862

863

864

865

866

867

868

869

Figure 1

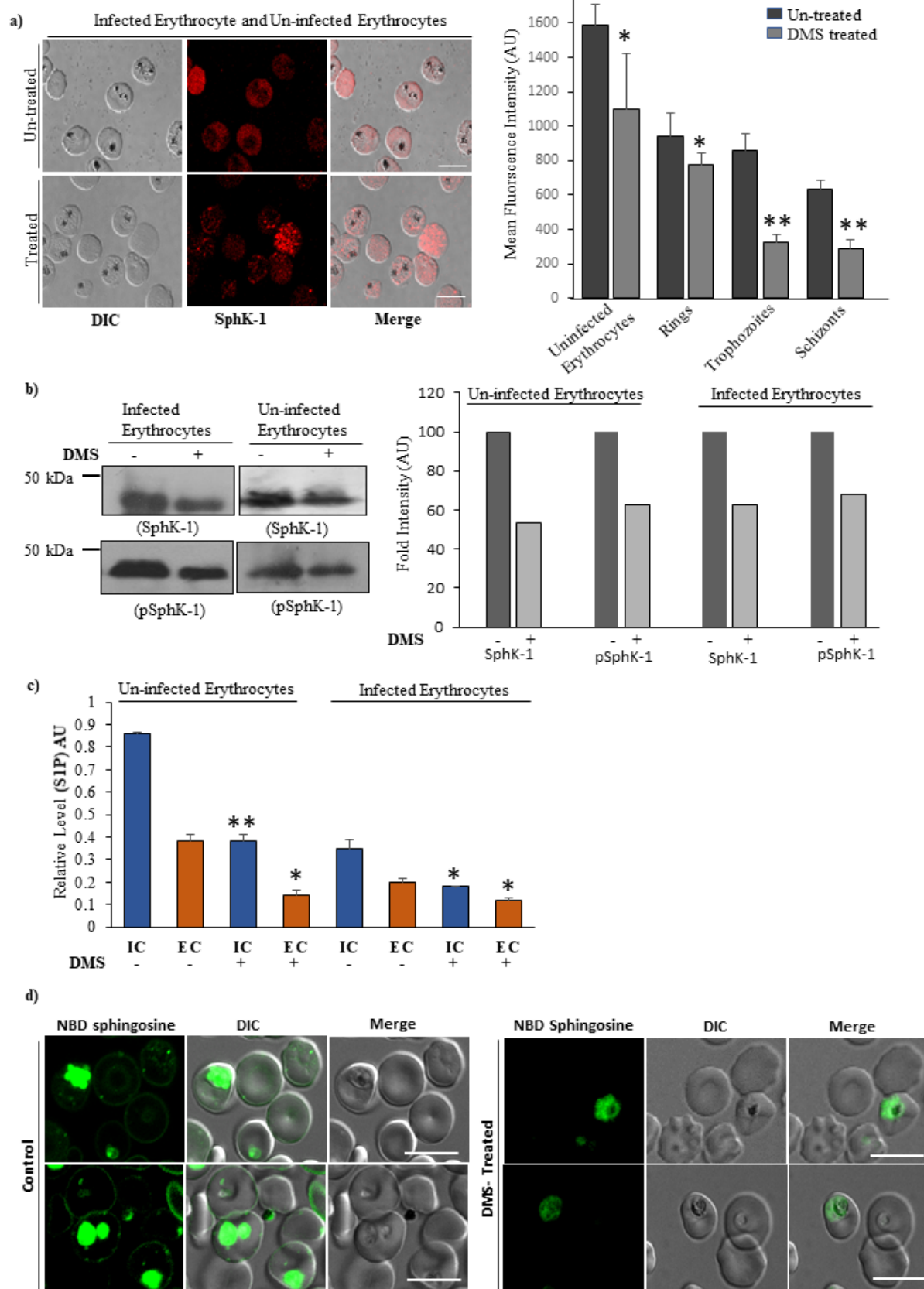


Figure 2

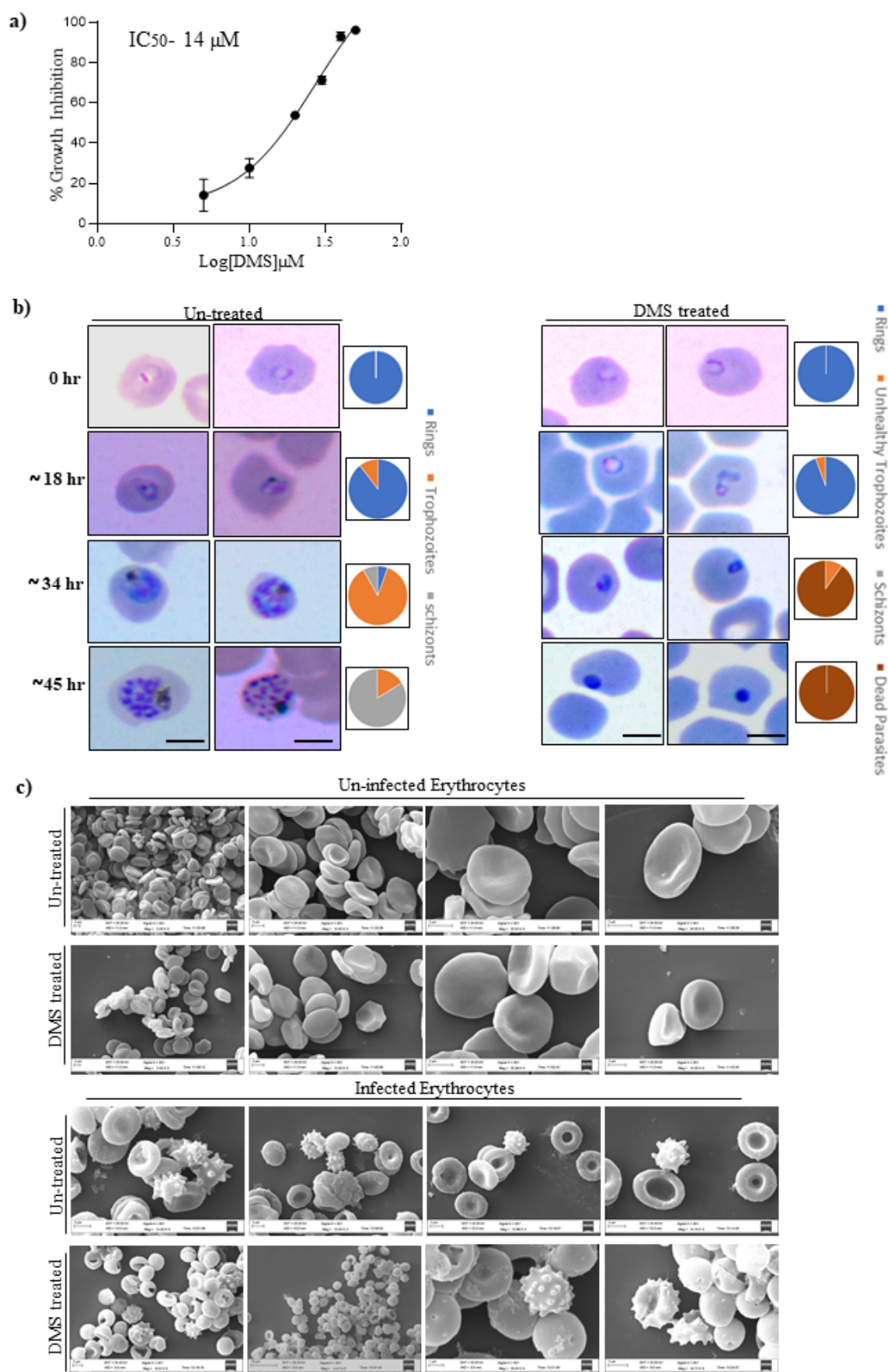


Figure 3

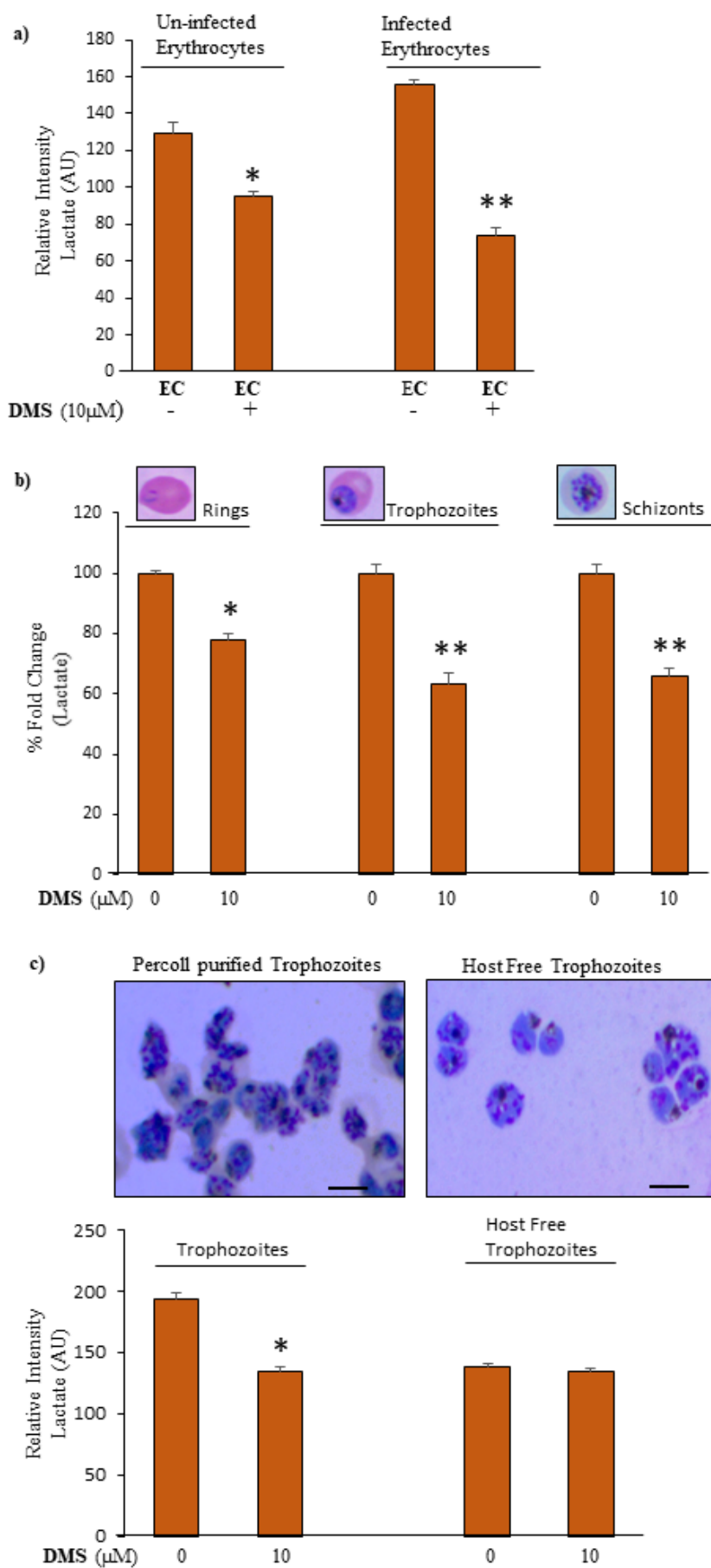
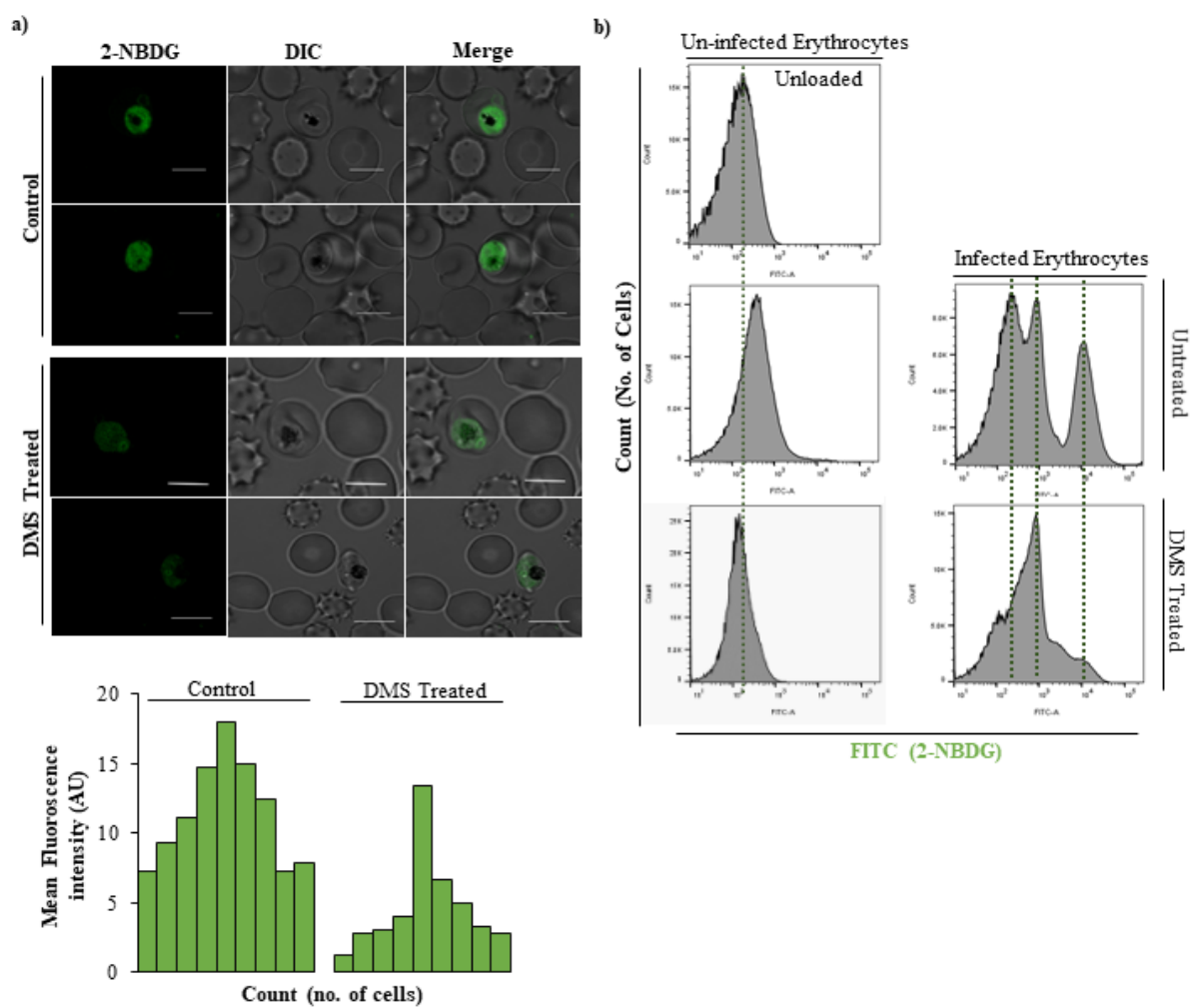


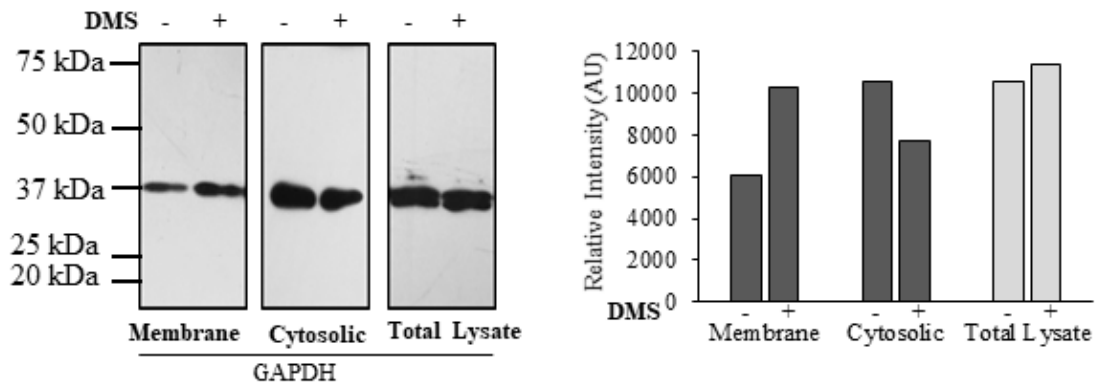
Figure 4



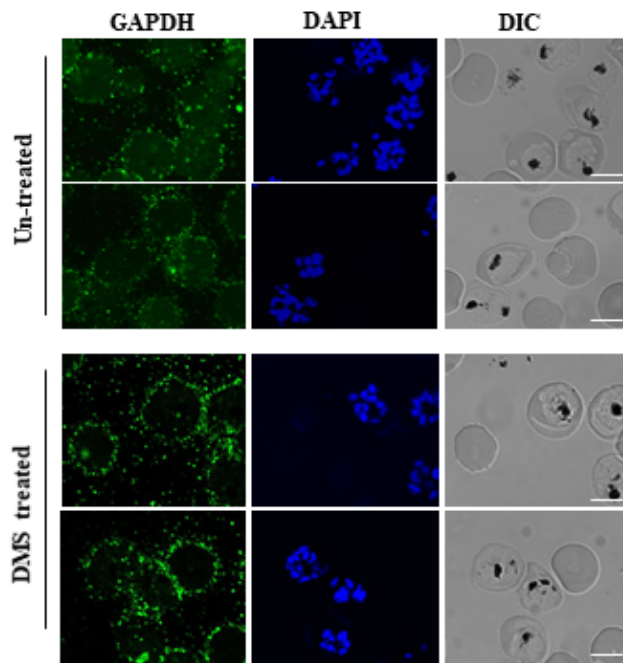
873

Figure 5

a)



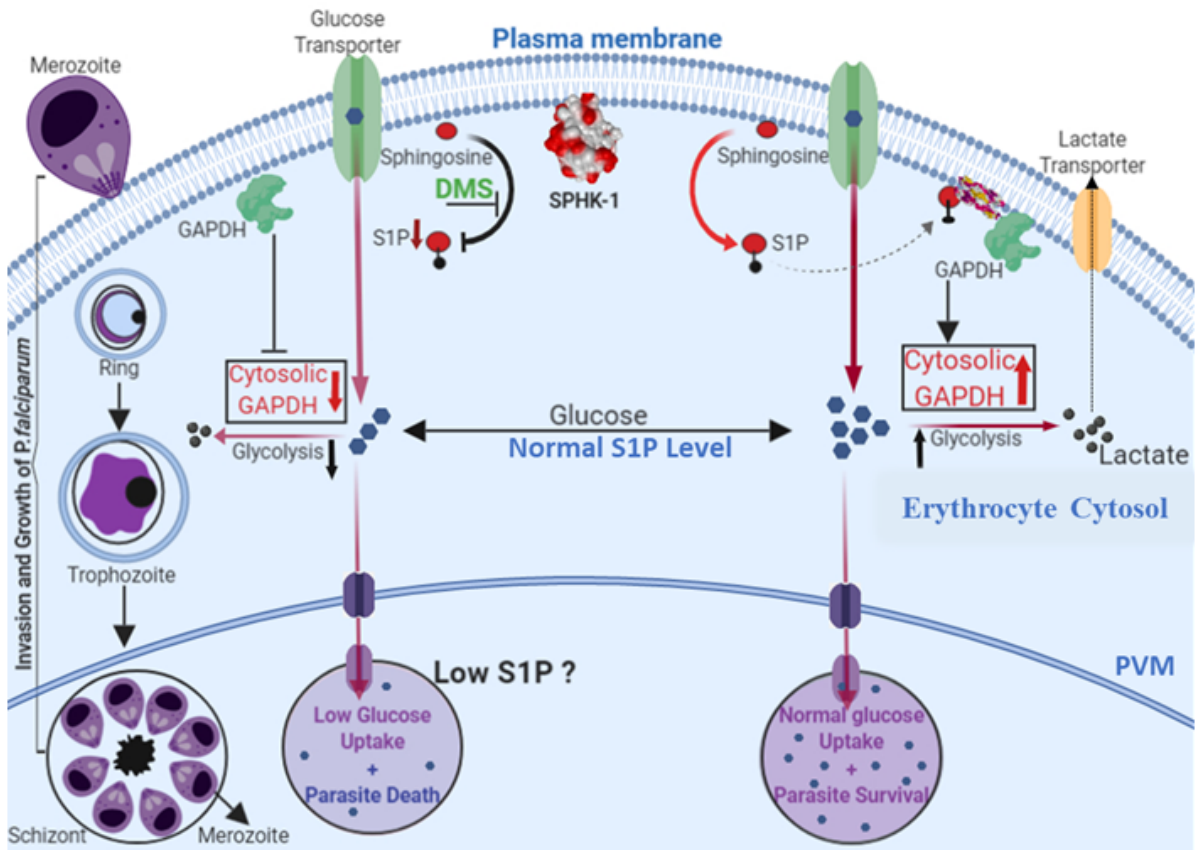
b)



874

Figure 6

a)



875

876